FRIGID ZONE **MEDICINE**
Original Article • DOI: 10.2478/fzm-2023-0014

Hydroxychloroquine induces long QT syndrome by blocking hERG channel

Xin Zhao[#], Lihua Sun[#], Chao Chen, Jieru Xin, Yan Zhang, Yunlong Bai, Zhenwei Pan, Yong Zhang, Baoxin Li, Yanjie Lv, Baofeng Yang[*]

Abstract

Objective: In March 2022, more than 600 million cases of Corona Virus Disease 2019 (COVID-19) and about 6 million deaths have been reported worldwide. Unfortunately, while effective antiviral therapy has not yet been available, chloroquine (CQ)/hydroxychloroquine (HCQ) has been considered an option for the treatment of COVID-19. While many studies have demonstrated the potential of HCQ to decrease viral load and rescue patients' lives, controversial results have also been reported. One concern associated with HCQ in its clinical application to COVID-19 patients is the potential of causing long QT interval (LQT), an electrophysiological substrate for the induction of lethal ventricular tachyarrhythmias. Yet, the mechanisms for this cardiotoxicity of HCQ remained incompletely understood. **Materials and methods:** Adult New Zealand white rabbits were used for investigating the effects of HCQ on cardiac electrophysiology and expression of ion channel genes. HEK-293T cells with sustained overexpression of human-ether-a-go-go-related gene (hERG) K^+ channels were used for whole-cell patch-clamp recordings of hERG K^+ channel current (I_{hERG}). Quantitative RT-PCR analysis and Western blot analysis were employed to determine the expression of various genes at mRNA and protein levels, respectively. **Results:** electrocardiogram (ECG) recordings revealed that HCQ prolonged QT and RR intervals and slowed heart rate in rabbits. Whole-cell patch-clamp results showed that HCQ inhibited the tail current of hERG channels and slowed the reactivation process from inactivation state. HCQ suppressed the expression of hERG and hindered the formation of the heat shock protein 90 (Hsp90)/hERG complex. Moreover, the expression levels of connexin 43 (CX43) and Kir2.1, the critical molecular/ionic determinants of cardiac conduction thereby ventricular arrythmias, were decreased by HCQ, while those of Cav1.2, the main Ca^{2+} handling proteins, remained unchanged and SERCA2a was increased. **Conclusion:** HCQ could induce LQT but did not induce arrhythmias, and whether it is suitable for the treatment of COVID-19 requires more rigorous investigations and validations in the future.

Keywords

COVID-19; hydroxychloroquine; LQT; hERG; Hsp90

Received 10 November 2021, accept 20 September 2022

Department of Pharmacology (State-Province Key Laboratories of Biomedicine-Pharmaceutics of China, Key Laboratory of Cardiovascular Medicine Research, Ministry of Education), College of Pharmacy, Harbin Medical University, Harbin 150086, China

**Corresponding author Baofeng Yang, E-mail: yangbf@hrbmu.edu.cn*
[#]These authors made equal contributions to this work.

1 Introduction

In March 2022, more than 600 million cases of coronavirus disease-19 (COVID-19) and about 6 million deaths have been reported worldwide[1]. The COVID-19 vaccines have been actively applied to the global community in the hope to prevent SARS-CoV-2 infection; however, the effectiveness of presently available vaccines can be jeopardized or compromised by evolving mutations of SARS-CoV-2. Therefore, the development of drugs to treat COVID-19 remains a top priority in combating the pandemic.

Recent reports indicated that the anti-inflammatory drugs, such as glucocorticoids and hydroxychloroquine (HCQ), and antiviral drugs, such as ivermectin and remdesivir, have been prescribed for the treatment of COVID-19, but their effectiveness is yet to be confirmed[2]. Chinese scholars have documented earlier that chloroquine (CQ), an antimalarial drug, can inhibit COVID-19 infection under *in vitro* conditions[3]. HCQ, a derivative of CQ, has a better safety profile than CQ[4-5]. The results from subsequent randomized clinical trials indicate that the combination of CQ or HCQ with azithromycin (AZM; an antibiotic medication) can effectively reduce mortality in

patients with COVID-19[6-7]. COVID-19 patients who received HCQ at an earlier stage had a better clinical outcome.

It has been reported that HCQ can block the invasion of SARS-CoV-2 into host cells by binding to angiotensin converting enzyme 2 (ACE2) receptors and subsequently blocking multiple processes of SARS-CoV-2 such as adsorption, invasion, synthesis, assembly and release *in vitro*[8-9]. HCQ also has anti-inflammatory and immune regulatory properties *via* affecting Toll-like receptor (TLR)-mediated signal transduction, which might be beneficial for COVID-19 patients[10-12]. However, increasing number of clinical studies has indicated that the therapeutic outcome of CQ/HCQ in COVID-19 patients is not different from that of placebo and could be even worse by increasing mortality[13-14]. HCQ has the potential to cause cardiotoxicity, ocular toxicity, ototoxicity, neuromuscular toxicity, and psychotoxicity[15-16]. Of note, the major cardiotoxicity induced by HCQ is manifested by long QT interval (LQT) (LQT) with an increased risk of torsades de pointes (TdP) (polymorphic ventricular tachycardia) or long QT syndrome (LQTS) leading to sudden cardiac death[17-18]. LQT after use of CQ/HCQ alone or co administration with AZM raises red flags for COVID-19 patients[19-20]. The polymorphic ventricular tachycardia or fibrillation, acute kidney failure, and resuscitated cardiac arrest have also been recorded in the patients under HCQ/AZM treatment[21]. Unfortunately, however, the mechanism by which HCQ causes LQT is currently uncertain though it is of paramount clinical importance and significance to delineate the underlying mechanism to mitigate the adverse effects and improve the clinical application of HCQ.

Previous computational and experimental studies have shown the inhibitory effect of HCQ on human ether-a-go-go-related gene (hERG)[22]. hERG encodes the alpha subunit of the cardiac rapid delayed rectifier K^+ current I_{Kr} that is responsible for the phase 3 rapid membrane repolarization of cardiac action potential[23]. hERG/I_{Kr} is known to be the major molecular and ionic mechanism underlying the acquired or drug-induced LQTS. The synthesis of hERG protein is regulated by many factors. It was found that the expression of hERG gene is controlled by the transcription factor Sp1 at the transcriptional level[24] and the transport of hERG channel proteins from cytoplasm to cell membrane is regulated by the heat shock proteins (Hsp) 70 and Hsp90 that serve as chaperone proteins during trafficking. hERG protein is also modified by the ubiquitin ligase Nedd4-2 and the niche protein caveolin (Cav1, Cav3) upon expression in the cell membrane, which enables the retrograde transport process of the membrane[25].

In this study, we investigated the effects of HCQ on hERG potassium channel activities in order to elucidate the ionic and molecular mechanisms for HCQ-induced LQT in rabbits. To this end, whole-cell patch-clamp techniques were employed in conjunction with molecular biology methods to measure the expression of hERG, junctional channel connexin-43 (Cx43), inward rectifier K^+ channel pore-forming α-subunit Kir2.1, Hsp70 and Hsp90, sarco/endoplasmic reticulum Ca^{2+}-ATPase sarco-endoplasmic reticulum ATPase 2a (SERCA2a), and L-type Ca^{2+} channel pore-forming α-subunit CaV1.2.

2 Materials and methods

2.1 Cell culture and reagents

Experiments were performed on HEK293T cells stably expressing hERG channel. Cells were cultured in Dulbecco's Modified Eagle Medium (DMEM, SH30022.01, Hyclone, Logan, Utah, USA) supplemented with 10% (v/v) fetal bovine serum (FBS, TBD15HT, TBD, Tianjin, China) and 1% penicillin-streptomycin (15070063, Gibco, MA, USA) under standard conditions at 37°C and 5% CO_2. For patch-clamp experiments, the cells were detached from culture dish by trypsin and were collected and stored at room temperature and used for subsequent patch-clamp recordings within 8 h.

HCQ was purchased from Aladdin company. HCQ at final concentrations of 1, 3, and 10 μmol/L was diluted with culture solution for patch-clamp experiments and with 0.9% NaCl solution for animal experiments.

2.2 Animals

Adult New Zealand white rabbits weighing between 2.1-2.9 kg were used in this study. The rabbits were provided by The Experimental Animal Center of Harbin Medical University (Grade II), China. The animals were conditioned at room temperature (23 ± 1°C) with a constant humidity (55% ± 5%) for a week and allowed for free access to food and tap water. The animals were housed individually in rabbit cages. The experimental protocol involving the animals was designed to minimize pain and discomfort to the animals in accordance with the guidelines of the China Council on Animal Care and Use and was approved by the Animal Ethical Committee of Harbin Medical University (IRB3023722).

2.3 Isolation of rabbit hearts

Upon completion of all experimental interventions or measurements, the rabbits were sacrificed by pushing air into the ear vein. After abdominal skin preparation, the upper abdomen of the rabbit was opened to expose the heart, which was quickly dissected out with surgical scissors and trimmed on an ice plate,

and then stored in a -80°C refrigerator for subsequent use.

2.4 Quantitative RT-PCR analysis

Total RNA was extracted using Trizol reagent (15596026CN, Invitrogen, MA, USA) and was then reverse transcribed. Quantitative RT-PCR was carried out on an ABI Prism 7500 System (Applied Biosystems Inc. USA). SYBR Green Gene Expression Assay (Qiagen, Valencia, CA) was used for *hERG*, *Cx43*, *Cav1.2*, *SERCA2a*, *Hsp70*, *Hsp90*, *Kir2.1* and *β-actin* expression. The sequences of the primer pairs used in our study were as following: *hERG*: 5′-CTTGCTGAAGGAGACGGAAG-3′ and 5′-GCGGAAGTTGATGAGGATGT-3′; *Cx43*: 5′-TTCTTGCTGATCC AGTGGTACATC-3′ and 5′-CAAGGACACCACCAGCATGA-3′; *Cav1.2*: 5′-TACCGTCAGTTCCACACAGC-3′ and 5′-CTTCAGAGT CAGGCAGAGCA-3′; *SERCA2a*: 5′-TTTTCCGTTACCTGGCTAT-3′ and 5′-CAGCATCCCATGTCAACAGA-3′; *Hsp70*: 5′-ACGTTTTGT TGAGTCCGTAA-3′ and 5′-GCTATATTCTTGTTAGGCAGC-3′; *Hsp90*: 5′-GCGACACCTGTTCATTGGACTGCTGATGGAT CTCC-3′ and 5′-GGAGATCCATCAGCAGTCCAATGAACAG GTGTCGC-3′; *Kir2.1*: 5′-ACCCGACAACAGTGCAGGAG-3′ and 5′-CAGCGGATGTCCACACAGGTA-3′; *β-actin*: 5′-ATTGCCGACAGGATGCAGAA-3′ and 5′-CAAGATCATTGCT CCTCCTGAGCGCA-3′. Fold changes were calculated using the formula $R=2^{-\Delta\Delta CT}$ for transcript quantification.

2.5 Western blot analysis

Protein levels were semi-quantified by Western blot analysis. The total protein samples were purified from rabbit heart tissues. Proteins were separated by SDS-PAGE. After electrophoresis, the proteins were transferred to PVDF membrane and incubated with 5% skim milk at room temperature for 2 h. The membrane was then incubated with primary antibodies and shaken in a 4°C swing bed overnight. The antibodies included SERCA2a (2A7-A1, Thermo, MA, USA), Cav1.2 (ab58552, Abcam, Cambridge, UK), Hsp70 (NB11096425, Novus, St. Louis, Missouri, USA), β-actin (abs137975, Absin, Shanghai, China). The membranes were then washed with 0.05% Tris-Buffered Saline with Tween-20 (TBST) 3 times with 10 min each time, incubated at room temperature for 1 hour with anti-rabbits/mouse secondary antibodies (926-32210 and 926-32211, Li-CoR, Lincoln, Nebraska USA) and washed 3 times with 0.05% TBST in the dark. Immunoblot images were captured, and band intensities were analyzed using the Odyssey system (Li-COR, USA).

2.6 Whole-cell patch-clamp recording techniques

The hERG K^+ current (I_{hERG}) was recorded in a whole-cell configuration at a voltage-clamp mode. The heat-polished patch pipette was filled with a pipette solution containing 0.1 mmol/L GTP (pH 7.3 KOH), 130 mmol/L KCl, 5 mmol/L Mg-ATP, 5 mmol/L EGTA, 1 mmol/L $MgCl_2 \cdot 6H_2O$, and 10 mmol/L HEPES. The pipette resistance was 2-4 MΩ. The extracellular solution contained 136 mmol/L NaCl, 5.4 mmol/L KCl, 5 mmol/L HEPES, 1 mmol/L $MgCl_2 \cdot 6H_2O$, 1 mmol/L $CaCl_2$, and 10 mmol/L glucose (pH 7.4 NaOH). The HCQ-containing extracellular solution was prepared freshly prior to electrophysiological recordings.

In electrophysiological recording, the maximum confluent cells were used after controlling the seeding density to 1-4 × 10^5 cells/flask and culturing for 1-3 days. Following treatment with 0.25% trypsin and 0.02% EDTA, the cells were transferred into the perfusion chamber installed on the stage of an inverted microscope and superfused with the extracellular solution at a rate of 1.5 mL/min (ix-70, Olympus, Tokyo). Axon 200B amplifier (Axon Axopatch 200B, Axon, New York, USA) was used to record I_{hERG}. Clampex pClamp 9 software (Molecular Devices, Sunnyvale, USA) was used to optimize capacitance compensation and series resistance compensation. The data were recorded on a computer by Digidata 1322A (Molecular Devices, Sunnyvale, USA).

2.7 ECG measurement in rabbits

According to the treatment protocol for novel coronavirus pneumonia (trial version 8) issued by the Chinese Health Care Commission, the recommended dosage of chloroquine is 500 mg/person/day. The drug conversion factor between human and rabbit is 3.27; therefore, rabbits were given HCQ at 25 mg/kg/day in the present study. Six days after HCQ administration, rabbits were fixed on the back position on a dissection table and allowed for calming down for 20 min. Electrocardiogram (ECG) was continuously recorded, and P wave, QRS complex, T wave amplitude, P-R, R-R and Q-T intervals were measured. Heart rates were also calculated.

2.8 Statistical analyses

Data are presented as mean ± standard error of mean (SEM). SPSS 22.0 Software (SPSS, Chicago, USA) was used for statistical analysis to evaluate the statistical differences. Student's t-test was used for comparisons between two groups, and one-way or two-way analysis of variance (ANOVA) was used to analyze statistical differences between groups under multiple different conditions. *P* values of < 0.05 (two-tailed) were considered statistically significant. Boltzmann function was used to fit the voltage-dependent activation and inactivation curves, and a single exponential function was used to fit the inactivation recovery curve. The data were analyzed by GraphPad Prism 8.0 (GraphPad, Santiago, USA).

3. Results

3.1 HCQ blocks the hERG potassium channel

It was well known that acquired or drug-induced QT prolongation is primarily related to the inhibitory activity of hERG potassium channel[26]. To elucidate the potential ionic mechanism by which HCQ prolongs QT interval, we first examined the effects of HCQ on hERG currents (I_{hERG}) in hERG-HEK293T cells by whole-cell patch-clamp techniques. The step I_{hERG} was elicited by a series of test pulses from -60 mV to +40 mV in 10 mV increments from a holding potential of -80 mV. The duration of each test pulse was 3.25 s, with an inter-pulse interval of 8 s, and each test pulse was followed by a repolarization step to -50 mV to induce an outward tail I_{hERG} with a slow decaying process. I_{hERG} was first recorded under control conditions, and then repeated following 10 min superfusion with HCQ at 24.0 ± 0.5°C. As shown in Fig. 1, HCQ produced concentration-dependent suppression of tail I_{hERG} (Fig. 1B) with minimal effect on the step currents (Fig. 1A) at concentrations of 1, 3 and 10 μmol/L. The I-V curves further revealed that (Fig. 1B) HCQ inhibited the tail I_{hERG} essentially at all test potentials examined (Fig. 1B).

3.2 HCQ accelerates inactivation of hERG channel

Many drugs block I_{hERG} in a gating-dependent manner by preferentially acting on the activated or inactivated state of hERG channels, the so-called open channel blockade or closed channel blockade. To clarify the possible state-dependency of action, we first investigated the effect of HCQ on the steady-state voltage-dependent activation properties of hERG channel. The activation curves (Fig. 2A) were constructed by normalizing the peak tail currents recorded from various pre-pulse potential to the maximum tail current elicited from a pre-pulse potential of -60 mV as shown in Fig. 1A and plotting the normalized current amplitude against the pre-pulse potentials. The normalized data (conductance) points were then fitted to a Boltzmann function. The results demonstrated that the threshold voltage for hERG channel activation was around -50 mV, and the half maximum activation voltage (V_{50}) was approximately 0.6 mV under control conditions, and HCQ caused a small positive shift of V_{50} to 1.6 mV (Fig. 2B). HCQ had no significant effects on the slope factor of the steady-state activation property of hERG channel.

On the other hand, the inactivation properties of hERG channels were assessed by analyzing I_{hERG} elicited with protocols shown in the inset of Fig. 2C. HCQ caused significant inhibition of I_{hERG} with conditioning voltages negative to -60 mV but did not alter I_{hERG} at more positive potentials, indicating that HCQ preferentially acts on the open state of hERG channels (Fig. 2D). Steady-state voltage-dependent inactivation curves of hERG were constructed by normalizing the peak currents at the test potential to the maximum current amplitude from a conditioning pulse at -120 mV and plotting the normalized currents against the potentials of conditioning pulses. The data were then fit to Boltzmann distribution. As illustrated in Fig. 2E and F, HCQ did not affect the voltage-dependent inactivation properties of hERG channels.

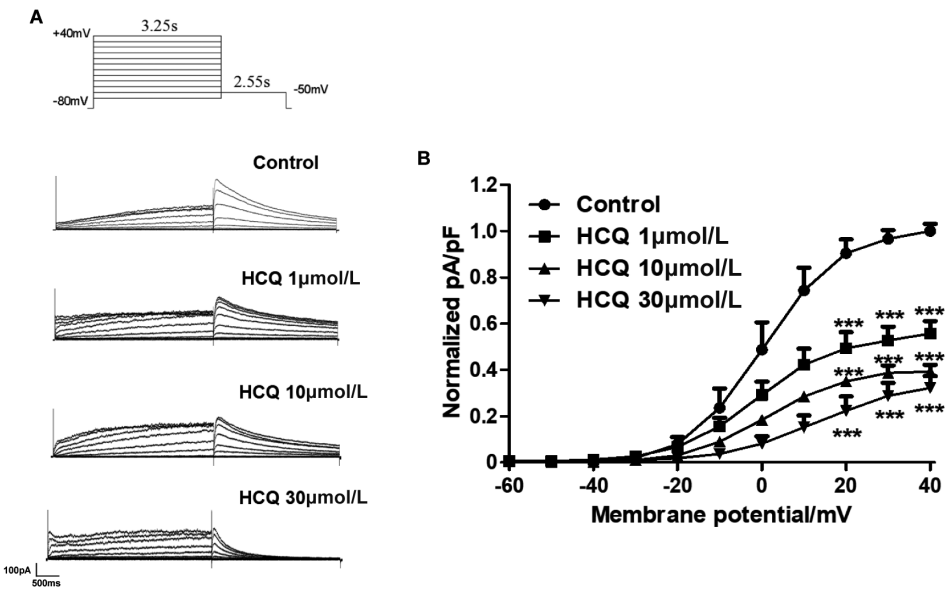

Fig. 1 HCQ blocks the hERG potassium channel current (I_{hERG}) in hERG-overexpressing HEK293T cells (hERG-HEK293T)

(A) Whole-cell voltage-clamp protocol and representative hERG current traces recorded from different experimental groups after expose of 1, 3, and 10 μmol/L HCQ. (B) Normalized I-V relationships for tail current in the presence of HCQ. $N = 6$, $^{***}P < 0.001$ *vs.* control.

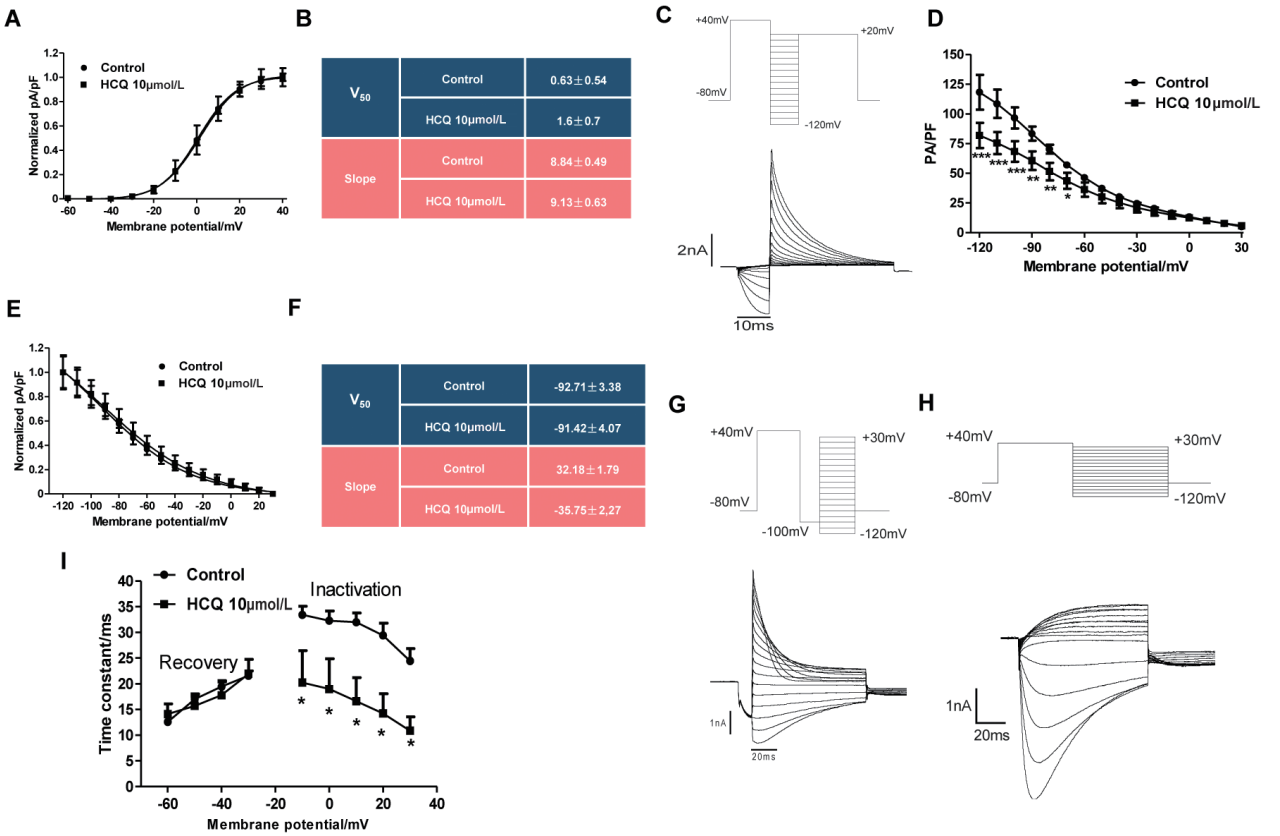

Fig. 2 The effect of HCQ on hERG channel kinetics in hERG-overexpressing HEK293T cells (hERG-HEK293T)

(A) Voltage-dependent activation curves for the control cells and the cells after exposure to HCQ for 24 h and the V_{50} and (B) slope value. (C) Whole-cell voltage-clamp protocol and representative current tracing for steady-state inactivation. (D) I-V relationships for inactivation current in the presence of HCQ. (E) The effect of HCQ on inactivation curve after incubated for 24 h and the V_{50} and (F) slope value. (G) Voltage-clamp protocol and representative current tracing for the onset of inactivation. (H) Voltage-clamp protocol and representative current tracing for the recovery from inactivation. (I) The effect of HCQ on the time constants of inactivation and recovery from inactivation after incubation for 48 h. Data are presented as mean ± SEM $N = 6$, $^{*}P < 0.01$, $^{**}P < 0.05$, $^{***}P < 0.001$ *vs.* control.

We next evaluated the effects of HCQ on the inactivation and reactivation kinetics of hERG channels (Fig. 2G-I). Notably, HCQ accelerated the inactivation process as reflected by the significant shortening of the inactivation time course or decrease in inactivation time constant without altering the reactivation time constant.

3.3 HCQ induces LQTs in animal models

Previous study has shown that QTc was prolonged in COVID-19 patients treated with HCQ[27]. Consistently, in our rabbit model, QT interval and corrected QT interval calculated based on Bazett's formula (QTcB) were both substantially lengthened by HCQ relative to those in the non-treated control group (Fig. 3A and B). Additionally, administration of HCQ also prolonged RR interval (Fig. 3D-F), indicating a slowing of cardiac conduction. Furthermore, HCQ decreased the heart rate (Fig. 3G). Yet, no arrhythmias were observed with HCQ treatment, neither was sudden cardiac death in our model.

The long-term blocking effect of I_{hERG} of HCQ was verified in hERG-HEK293T cells treated with HCQ for 48 h. As depicted in Fig. 3H and I, HCQ produced concentration-dependent inhibition of hERG tail currents at 1, 10 and 30 μmol/L.

3.4 Effects of HCQ on cardiac ion channels and their regulatory proteins

The mRNA level of ERG channels in the rabbit heart was found enormously reduced after 6 days of HCQ treatment, indicating that HCQ repressed the transcription of rabbit ERG gene (Fig. 4A). It is known that the maturation of hERG channel proteins following synthesis requires the presence of heat-shock proteins 70 and 90 (Hsp70 and Hsp90), the cytosolic chaperones, that play important roles in regulating the transport of hERG channel

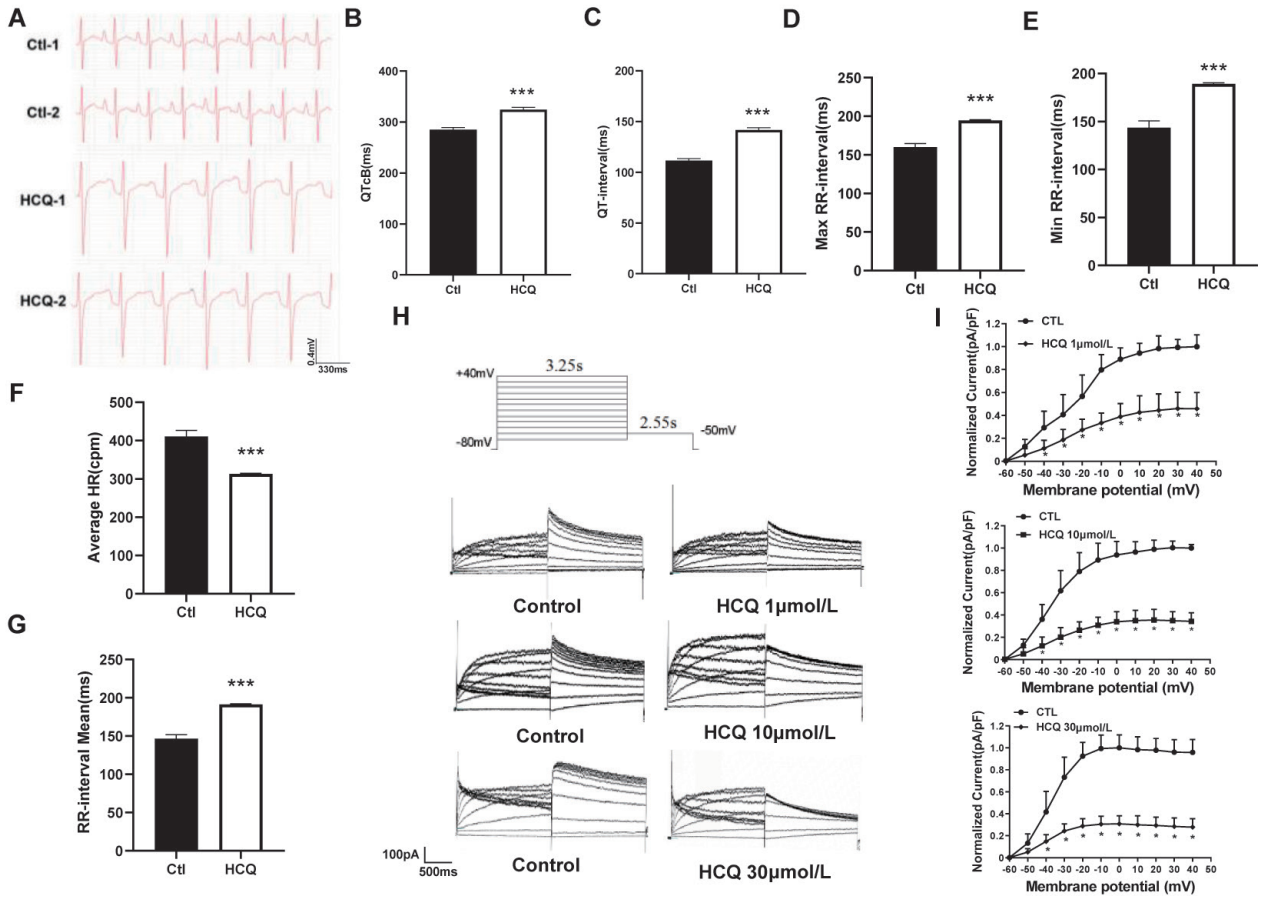

Fig. 3 The effects of HCQ on cardiac electrophysiology

(A) The representative diagram of ECG in rabbits. (B-G) HCQ prolongs QTc (B), QT interval (C) and max-RR interval (D), min-RR interval (E), mean RR interval (F) and decreases heart rate (G) in rabbit heart. (H-I) Whole-cell voltage-clamp protocol and representative hERG current traces recorded from hERG-HEK293T cell line treated with 1, 3, and 10 μmol/L HCQ. Normalized I-V relationships for tail current in the presence of HCQ. $N = 6$, $^{*}P < 0.01$, $^{***}P < 0.001$ *vs.* control.

proteins to the cytoplasmic membrane[28]. Our experiments uncovered that HCQ reduced the mRNA level of HSP90, but not HSP70 (Fig. 4B-D).

The lengthening of RR interval in the presence of HCQ suggests that this compound might also affect cardiac conduction in addition to repolarization. To test this notion, we evaluated the effects of HCQ on the expression of intercellular gap junction channel Cx43 that determines the intercellular propagation of cardiac impulses (Fig. 4E) and inward rectifying K^+ channel Kir2.1 that sets the resting membrane potential to control cardiac conduction (Fig. 4F) was decreased after HCQ treatment.

On the other hand, SERCA2a, the main intracellular Ca^{2+} handling proteins, was increased (Fig. 4G and H) and Cav1.2 was not changed significantly by HCQ (Fig. 4I and J).

4 Discussion

A series of three major epidemics of human coronavirus have already been recorded in the past 20 years: severe acute respiratory syndrome (SARS)[29] in 2002, Middle East respiratory syndrome (MERS)[30] in 2012[31], and COVID-2019[32]. The symptoms of SARS typically include fever, chills, and body aches, and the onset of pneumonia, with a fatality rate of about 9.6%. According to the available data on a global basis, the fatality rate of COVID-19 is about 4.9%[33]. While coronaviruses have been around for decades, there have been no effective antiviral drugs against them, and coronaviruses remain a serious life-threatening pathogen to humans. Hence, only a high-dose glucocorticoid shock therapy may be applied clinically to suppress the immune system and rescue the patients' lives[34]. Based on follow-up investigations that lasted for decades, it was found that many of the symptoms of SARS patients are similar to those of COVID-19, including

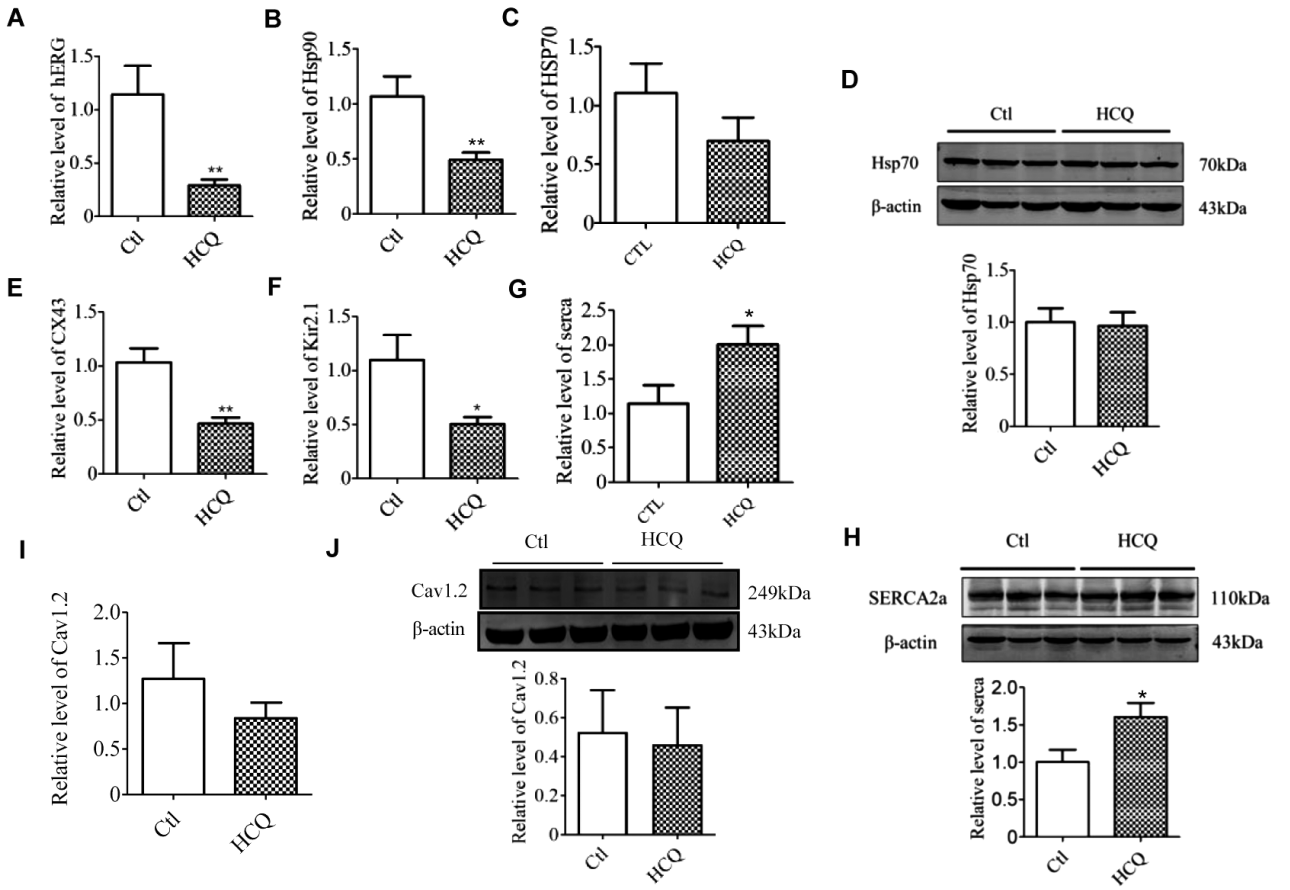

Fig. 4 Effects of HCQ on the expression of cardiac ion channels and their regulatory proteins in rabbit hearts

(A) Relative mRNA level after HCQ administration for 1 week. HCQ incubation remarkably reduced the mRNA level of hERG and had no effect on (B) Hsp90 and (C) HSP70. (D) Western blots results and statistics of HSP70 expression. HCQ incubation does not decrease the expression level of Hsp70. (E-H) Relative mRNA or protein level after HCQ administration for 1 week. HCQ incubation remarkably reduced the mRNA level of (E) Cx43 and (F) Kir2.1 and increased the expression of (G-H) SERCA2a and had no effect on (I-J) CaV1.2. $N = 5\text{-}7$, $^{*}P < 0.01$, $^{**}P < 0.05$ *vs*. control.

sequelae such as osteoporosis, femoral head necrosis, and pulmonary fibrosis after being cured[35]. It is a good correlation between the SARS symptoms and the glucocorticoids that were being frequently prescribed at that time. To avoid such a problem and minimize toxic side effects derived from pharmacological therapy, various drugs in the market have been screened for their efficacy against SARS-CoV-2 and better safety profiles, and HCQ is considered one of the choices for safer treatment of COVID-19.

HCQ belongs to 4-aminoquinoline derivative antimalarial drugs and has similar pharmacological effects and mechanisms to chloroquine but its toxicity was believed to be only half of that of chloroquine. Even though, the side-effects of HCQ are still a great concern; of note, cardiotoxicity is the most commonly reported side-effect of this compound. Therapy with HCQ became the standard routine in many hospitals in the early stages of the COVID-19 epidemic. The U.S. Food and Drug Administration (FDA) has authorized the emergency use of CQ and HCQ for patients with COVID-19. However, no large, randomized trials have thus far demonstrated the clinical efficacy of HCQ or HCQ in combination with azithromycin for the treatment of COVID-19. On the contrary, there has been growing evidence that HCQ is not highly beneficial in the management of COVID-19. The therapeutic feasibility of HCQ for COVID-19 remains a matter of controversy with many clinical trials reporting contradictory outcomes[36-38]. To better understand the cardiotoxicity of HCQ for the management of patients with COVID-19, we performed the present study.

Our study uncovered that HCQ produces LQT in rabbits that naturally express sizeable I_{hERG}, likely by blocking I_{hERG} in HEK293T cells engineered to overexpress hERG channels. This finding is in

good agreement with the results from clinical application of HCQ to COVID-19 patients. LQT is characterized by a prolonged QT interval and aberrant T waves on the electrocardiogram. Prolonged QT interval is associated with patient syncope and may lead to sudden cardiac death due to tip-twist ventricular tachycardia[39]. LQT provoked by drugs such as HCQ was called acquired LQT, and there was no clinically effective treatment drug for this type of arrhythmia. The incidence of drug-induced LQT commonly correlates with the inactivation of hERG channels[40]. Here, we found that HCQ inhibits hERG activity by functionally blocking I_{hERG}, transcriptionally repressing hERG expression, and post-translationally interfering hERG trafficking (*via* repressing HSP90 expression). The findings explain for the LQT induced by HCQ.

Despite the significant QT prolongation in the presence of HCQ, we observed no ventricular arrhythmias in rabbis under our experimental conditions. This could be explained by our findings that HCQ did not affect SERCA2a and CaV1.2. It is known that two requirements need to be fulfilled in order for arrhythmias to be initiated, arrhythmic substrate and arrhythmic trigger. For torsade de pointes, QT prolongation is the substrate and abnormal inward currents (*e.g.*, Ca^{2+} inflow) during the plateau phase of an action potential is the trigger. In our study, while HCQ generated the substrate, it did not enhance CaV1.2 nor suppress SERCA2a indicating that the arrhythmic trigger remined unaltered.

On the other hand, our data demonstrated that HCQ repressed the expression of Cx43 and Kir2.1, indicating that this agent might also cause cardiac conduction slowing in addition to QT prolongation. Our study therefore identified a new mechanism for the cardiotoxicity of HCQ in terms of cardiac electrophysiological disturbances. Nonetheless, QT prolongation by HCQ could increase effective refractory period (ERP), which might offset the arrhythmogenic potential conferred by conduction slowing.

Evidently, HCQ induces multiple electrophysiological disorders by multiple ionic/molecular mechanisms that interplay to offset one another the arrhythmogenic or proarrhythmic potential. This notion might be further extended to explain the non-fatal cardiotoxicity of HCQ in COID-19 patients. However, the potential for using HCQ in COVID-19 patients with other co-morbidities needs to be further evaluated. Overall, in spite of the evidence from some clinical trials that HCQ may save the lives of patients suffering from COVID-19, its relevance for the treatment of COVID-19 deserves to be discussed because of its LQT-inducing side effects and other as yet unknown adverse effects.

Author contributions

Zhao X and Sun L H made equal contributions to this work. All authors contributed to the interpretation of data, critical revision of the manuscript, and provided final approval of the submitted and published version.

Ethnical Approval

The experimental protocol involving the animals was designed to minimize pain and discomfort to the animals in accordance with the guidelines of the China Council on Animal Care and Use and was approved by The Animal Ethical Committee of Harbin Medical University (IRB3023722).

Conflicts of interests

Yang B F is the chief editor of the journal. The article was subject to the journal's standard procedures, with peer review handled independently of this member and his research groups.

References

[1] Filchakova O, Dossym D, Ilyas A, *et al.* Review of COVID-19 testing and diagnostic methods [J]. Talanta, 2022; 244: 123409.
[2] Trivedi N, Verma A, Kumar D. Possible treatment and strategies for COVID-19: review and assessment. Eur Rev Med Pharmacol Sci, 2020; 24(23): 12593-12608.
[3] Wang M, Cao R, Zhang L, *et al*. Remdesivir and chloroquine effectively inhibit the recently emerged novel coronavirus (2019-nCoV) *in vitro*. Cell Res, 2020; 30(3): 269-271.
[4] Jorge A, Ung C, Young L, *et al.* Hydroxychloroquine retinopathy - implications of research advances for rheumatology care. Nat Rev Rheumatol, 2018; 14(12): 693-703.
[5] McChesney E W. Animal toxicity and pharmacokinetics of hydroxychloroquine sulfate. Am J Med, 1983; 75(1a): 11-18.
[6] Gautret P, Lagier J C, Parola P, *et al*. Hydroxychloroquine and azithromycin as a treatment of COVID-19: results of an open-label non-randomized clinical trial. Int J Antimicrob Agents, 2020; 56(1): 105949.
[7] Borba M G S, Val F F A, Sampaio V S, *et al.* Effect of high *vs.* low doses of chloroquine diphosphate as adjunctive therapy for patients hospitalized with severe acute respiratory syndrome coronavirus 2 (SARS-CoV-2) infection: a randomized clinical trial. JAMA Netw Open, 2020; 3(4): e208857.
[8] Vincent M J, Bergeron E, Benjannet S, *et al.* Chloroquine is a potent inhibitor of SARS coronavirus infection and spread. Virol J, 2005; 2:69.
[9] Lescure F X, Bouadma L, Nguyen D, *et al.* Clinical and virological

data of the first cases of COVID-19 in Europe: a case series. Lancet Infec Dis, 2020; 20(6): 697-706.
[10] In't Veld A E, Jansen M A A, Ciere L C A, *et al.* Hydroxychloroquine effects on TLR signaling: Under exposed but unneglectable in COVID-19. J Immunol Res, 2021; 6659410.
[11] Torigoe M, Sakata K, Ishii A, *et al.* Hydroxychloroquine efficiently suppresses inflammatory responses of human class-switched memory B cells *via* Toll-like receptor 9 inhibition. Clin Immunol, 2018; 195: 1-7.
[12] Meo S A, Klonoff D C, Akram J. Efficacy of chloroquine and hydroxychloroquine in the treatment of COVID-19. Eur Rev Med Pharmacol Sci, 2020; 24(8): 4539-4547.
[13] Lopez A, Duclos G, Pastene B, *et al.* Effects of hydroxychloroquine on COVID-19 in intensive care unit patients: preliminary results. Int J Antimicrob Agents, 2020; 56(5): 106136.
[14] Molina J M, Delaugerre C, Le Goff J, *et al.* No evidence of rapid antiviral clearance or clinical benefit with the combination of hydroxychloroquine and azithromycin in patients with severe COVID-19 infection. Med Mal Infect, 2020; 50(4): 384.
[15] Good M I, Shader R I. Lethality and behavioral side effects of chloroquine. J Clin Psychopharmacol, 1982; 2(1): 40-47.
[16] Al-Bari M A. Chloroquine analogues in drug discovery: new directions of uses, mechanisms of actions and toxic manifestations from malaria to multifarious diseases. J Antimicrob Chemother, 2015; 70(6): 1608-1621.
[17] Doyno C, Sobieraj D M, Baker W L. Toxicity of chloroquine and hydroxychloroquine following therapeutic use or overdose. Clin Toxicol (Phila), 2021; 59(1): 12-23.
[18] Yendrapalli U, Ali H, Green J L, *et al.* Effects of cardiac toxicity of combination therapy with hydroxychloroquine and azithromycin in COVID-19 patients. J Infect Public Health, 2021; 14(11): 1668-1670.
[19] Magagnoli J, Narendran S, Pereira F, *et al.* Outcomes of hydroxychloroquine usage in United States veterans hospitalized with Covid-19. medRxiv, 2020: 20065920.
[20] Rosenberg E S, Dufort E M, Udo T, *et al.* Association of Treatment With Hydroxychloroquine or Azithromycin With In-Hospital Mortality in Patients With COVID-19 in New York State. JAMA, 2020; 323(24): 2493-2502.
[21] Gopinathannair R, Merchant F M, Lakkireddy D R, *et al.* COVID-19 and cardiac arrhythmias: a global perspective on arrhythmia characteristics and management strategies. J Interv Card Electrophysiol, 2020; 59(2): 329-336.
[22] Yu R, Li P. Computational and experimental studies on the inhibitory mechanism of hydroxychloroquine on hERG. Toxicology, 2021; 458: 152822.
[23] Sanguinetti M C, Jiang C, Curran M E, *et al.* A mechanistic link between an inherited and an acquired cardiac arrhythmia: HERG encodes the I_{Kr} potassium channel. Cell, 1995; 81(2): 299-307.
[24] Zhang Y, Dong Z, Jin L, *et al.* Arsenic trioxide-induced hERG K^+ channel deficiency can be rescued by matrine and oxymatrine through up-regulating transcription factor Sp1 expression. Biochem Pharmacol, 2013; 85(1): 59-68.
[25] Lamothe S M, Zhang S. Chapter five - ubiquitination of ion channels and transporters. Prog Mol Biol Transl Sci, 2016; 141: 161-223.
[26] Mitcheson J S, Chen J, Lin M, *et al.* A structural basis for drug-induced long QT syndrome. Proc Natl Acad Sci U S A, 2000; 97(22): 12329-33.
[27] Oscanoa T J, Vidal X, Kanters J K, *et al.* Frequency of Long QT in Patients with SARS-CoV-2 Infection Treated with Hydroxychloroquine: A Meta-analysis. Int J Antimicrob Agents, 2020: 56(6): 106212.
[28] Anneken L, Baumann S, Vigneault P, *et al.* Estradiol regulates human QT-interval: acceleration of cardiac repolarization by enhanced KCNH2 membrane trafficking. Eur Heart J, 2016; 37(7): 640-650.
[29] Stadler K, Masignani V, Eickmann M, *et al.* SARS--beginning to understand a new virus. Nat Rev Microbiol, 2003; 1(3): 209-218.
[30] Chafekar A, Fielding B C. MERS-CoV: Understanding the latest human coronavirus threa. Viruses, 2018; 10(2): 93.
[31] Jartti T, Jartti L, Ruuskanen O, *et al.* New respiratory viral infections. Curr Opin Pulm Med, 2012; 18(3): 271-278.
[32] Ciotti M, Angeletti S, Minieri M, *et al.* COVID-19 Outbreak: An Overview. Chemotherapy, 2019; 64:215-223.
[33] He W, Yi G Y, Zhu Y. Estimation of the basic reproduction number, average incubation time, asymptomatic infection rate, and case fatality rate for COVID-19: Meta-analysis and sensitivity analysis. J Med Virol, 2020; 92(11): 2543-2550.
[34] Yaqoob H, Greenberg D, Hwang F, *et al.* Comparison of pulse-dose and high-dose corticosteroids with no corticosteroid treatment for COVID-19 pneumonia in the intensive care unit. J Med Virol, 2022; 94(1): 349-356.
[35] Wang W, Zhang N, Guo W, *et al.* Combined pharmacotherapy for osteonecrosis of the femoral head after severe acute respiratory syndrome and interstitial pneumonia: two and a half to fourteen year follow-up. Int Orthop, 2018; 42(7): 1551-1556.
[36] Elavarasi A, Prasad M, Seth T, *et al.* Chloroquine and hydroxychloroquine for the Treatment of COVID-19: a Systematic Review and Meta-analysis. J Gen Intern Med, 2020; 35(11): 3308-3314.
[37] Million M, Lagier J C, Gautret P, *et al.* Early treatment of COVID-19 patients with hydroxychloroquine and azithromycin: A retrospective analysis of 1061 cases in Marseille, France. Travel Med Infect Dis, 2020; 35:101738.
[38] Shah S, Das S, Jain A, *et al.* A systematic review of the prophylactic role of chloroquine and hydroxychloroquine in coronavirus disease-19 (COVID-19). Int J Rheum Dis, 2020; 23(5): 613-619.
[39] Kaufman E S. Arrhythmic risk in congenital long QT syndrome. J Electrocardiol, 2011; 44(6): 645-649.
[40] Zhou Z, Gong Q, January C T. Correction of defective protein trafficking of a mutant HERG potassium channel in human long QT syndrome. Pharmacological and temperature effects. J Biol Chem, 1999; 274(44): 31123-31126.